Diffusion Model Spread of Electric Charge in the Resistive Micromegas Detectors: Implementation to the New Small Wheel Upgrade of the ATLAS Experiment

T. Alexopoulos[a], M. Dris[a], S. Maltezos*[a], and G. Iakovidis[b]

[a]*National Technical University of Athens, Department of Physics, 15780 Athens, Greece*
[b]*Brookhaven National Laboratory, Upton, NY 11973, USA*

Abstract

Abstract. The study of the operation of the resistive Micromegas detector of the New Small Wheel upgrade of the ATLAS Experiment is presented in this work. The main prospect is the understanding of the spark suppression mechanism in the amplification region. Namely, the space-time solution of a point-like electric charge spread along a resistive strip is calculated analytically. For this purpose, the method of reflection and superposition was applied under the particular initial and boundary conditions. An appropriate methodology for the correct virtual image charges configuration is introduced. In addition, the electric field in the amplification region is calculated as a function of the deposited charge position and the resistance of the strip material, while the results are discussed.

Keywords— ATLAS Experiment, Resistive Micromegas, Charge density, Transient electric field, Diffusion.

1 Introduction

In the framework of ATLAS Muon Spectrometer upgrade, two New Small Wheel (NSW) detector systems, have been completed recently and are being installed in their foreseen locations in the ATLAS Cavern for Run 3. In this work we are concentrating on the Micromegas detectors [1, 2] of the two NSW, A and C, and more specifically to their operation for spark rate suppression based on the resistive strip layer. The geometrical end electrical details of the resistive strip configuration in conjunction with the readout strips are given analytically in [3, 4].

The technology of resistive Micromegas detectors is an invention where its various elements are optimised in a way that the electrical signal is not lost through the resistive layer but is propagated to the separate layer carrying the resistive strips and these two layers are capacitive coupled. Therefore, the readout electrode is not any more directly exposed to the charge created in the amplification region. The main mechanism for the spark suppression is the opposite direction of the created electric field, as it is described in the following sections. By this technique, the electric field released during spark formation is sufficiency reduced and thus the Micromegas detector becomes spark-insensitive. However, the highly ionizing particles, produced in the LHC collisions, leads to an increasing probability for spark occurrence. This reason was the motivation for the present study aiming to localize the crucial parameters which could specify an optimum design configuration.

In the present study we investigate the spreading mechanism of the deposited electric charge on the resistive strips as a general consideration referring to this signal forming technique. Nevertheless,

*Corresponding author: S. Maltezos, National Technical University of Athens, 15780 Athens, Greece, e-mail: maltezos@central.ntua.gr

in the implementation of the analysis we focus exclusively on the geometric characteristics of the structure of the NSW Micromegas.

In section 2 the spread mechanism in one dimension resistive strip and the corresponding solution is analytically described, in section 3 an extension to 2-D resistive strip is considered while the space-time electric field is calculated while a discussion regarding the obtained results is given. Finally, the conclusions and prospects are presented.

2 Space-time diffusion-like along 1-D strip

2.1 Formulation of the 1-D problem

Let us consider a resistive strip of length L by side view (longitudinal) above the corresponding readout strip. Their basic geometric configuration inside the amplification region including the mesh (or micromesh) electrode is presented in Fig. 1. The mesh electrode and the readout strips are connected to the common ground through the electronics. The resistive strip at the position $x = 0$ is floating (unconnected electrically). At the position $x = L$ it is connected together with all the other strips by the use of a conductor silver line which, in turn, is connected to the positive electrode (+HV) of the High Voltage power supply. In the first step of analysis we ignore its perpendicular dimension (along y) considering it as one- dimensional (1-D) strip. At time $t = 0$ we assume that an electric point-like charge cluster (or simply "point charge" used in the next) Q is deposited instantaneously on a resistive strip at an arbitrary position $x = x_0$.

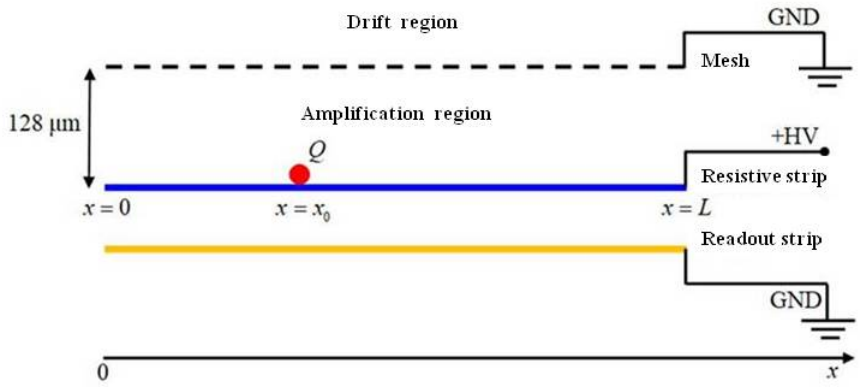

Figure 1: A schematic representing the resistive strip location among with the readout strips and the mesh electrode in the amplification region of Micromegas detector - not in scale. An electric point charge (red solid circle) is deposited at an arbitrary position and starts to be diffused in both directions along the strip.

The deposited point charge Q, essentially is a cluster of electrons emerging from the drift region and multiplying in the amplification region, can be spread along the one-dimensional resistive strip in both directions, $x < x_0$ and $x > x_0$ within the maximum length, $x_{max} = L$. This point charge creates an one-dimensional space-time charge density along the resistive strip [5, 6]. At $x = 0$ the charge is considered to be impermeable (because the left end is floating - in air) specifying the corresponding boundary condition of this closed electrical system. At $x = L$ (right end of the strip) the distributed charge reaching this position is lost by neutralization due to the connection to the conductor silver line and to +HV terminal acting as a "sink", that is, the charge density should be $\rho(L, t) = 0$. The Partial Differential Equation (PDE) describing the charge spread mechanism is the well-known "Telegraph" equation [7]. This PDE for very low inductance per unit length, as is the case in the resistive strips, approximately takes the form of a diffusion-like equation. A charge decay term is included coming from a non-zero conductance per unit length expressed by the decay constant rate α, as it is also described analytically in [8]

$$\frac{\partial \rho(x,t)}{\partial t} = D\frac{\partial^2 \rho(x,t)}{\partial x^2} - a\rho(x,t) \tag{1}$$

where $D = 1/RC$ is the a constant playing the role of a diffusion constant, R being the resistivity per unit length and C the equivalent overall capacitance per unit length. The constant $\alpha > 0$ is an assumed decay constant rate which is included to cover the most general case. In a typical case of our application we have: $R = 8$ MΩ/cm, $C = 100$ pF/m and thus, $D = 1/\left(8\ \text{MΩ/cm} \cdot 100\text{pF/m}\right) = 1/8\ \text{cm}^2/\mu\text{s}$.

The typical length of a resistive strip is $L = 100$ cm, while in the present study we consider as a deposited point charge $Q = 16$ pC which, according to [9], creates a transient electric field for which its component in the perpendicular direction is equal and opposite of the constant electric field applied in the amplification region, which is typically 570 V/128 μm = 44.5 kV/cm. This assumption constitutes a reference while the actual value levels of the charge will be investigated based on experimental data regarding the NSW Micromegas detectors.

Under these conditions sparking can stop but since the total charge is diffused and decreased by time, the electric field will change as a function of time accordingly and is also reduced progressively. The total charge decreasing rate, surely, is not governed by a exponential discharge of a simple RC circuit, in readily is more complicate as it is given in the solution we are investigating. However, a rough estimate of the decay time could be the time constant $\tau' = R'C'$, where $R' = R(L - x_0)$ and $C' = CL$ or equivalently, $\tau' = RC(L - x_0)L$. A more representative time span, an "equivalent decay time" of the total charge and the associated field is proposed. This is the time for total charge reduction at the value $Q/e = 0.369Q$, corresponding to a decay time of a hypothetical exponential decreasing function. Alternatively, we use the "equivalent half-time" for total charge reduction at the value $Q/2$.

2.2 Solution for the 1-D problem

Returning to the theoretical consideration and taking into account the described dynamical "picture", the initial and boundary conditions for the PDE are described as follows:

a) Initial condition for $t = 0$

   1) $\rho(x,0) = Q\delta(x - x_0)$

b) Boundary conditions at left and right ends

   1) $\left.\frac{\partial \rho(x,t)}{\partial x}\right|_{x=0} = 0$ (Neumann)
   2) $\rho(x,t)|_{x=L} = \rho(L,t) = 0$ (Dirichlet)

where $\delta(x - x_0)$ is the Dirac function at position $x = x_0$. We must point out that in the position of boundary condition b-1 we expect to have a negative slope of the charge density for every time t, $\left.\frac{\partial \rho(x,t)}{\partial x}\right|_{x=L} = -\lambda(t)$, where $\lambda(t)$ is a positive defined function of time. It expresses the temporal rate of charge drop in this position and can be determined after finding the solution of the problem.

The solution of the PDE Eq. 1 for $\rho(x,t)$, based on diffusive Malthus equation [10] is given by

$$\rho(x,t) = e^{-at}\frac{Q}{\sqrt{4\pi Dt}}e^{-(x-x_0)^2/4Dt} = \frac{Q}{\sqrt{4\pi Dt}}e^{-\left[at+(x-x_0)^2/4Dt\right]}$$

This space-time function is of a Gaussian shape spreading and decreasing by time due to the exponential factor, The total charge, Q_t, as a function of time is given by

$$Q_t(x,t) = \int_0^L \frac{Q}{\sqrt{4\pi Dt}} e^{-\left[at+(x-x_0)^2/4Dt\right]} \mathrm{d}x = \frac{Qe^{-at}}{\sqrt{4\pi Dt}} \int_0^L e^{-(x-x_0)^2/4Dt} \mathrm{d}x$$

$$= \frac{\sqrt{4Dt}Qe^{-at}}{\sqrt{4\pi Dt}} \int_0^{(L-x_0)/\sqrt{4Dt}} e^{-y^2} \mathrm{d}y = \frac{Qe^{-at}}{\sqrt{\pi}} \int_0^{(L-x_0)/\sqrt{4Dt}} e^{-y^2} \mathrm{d}y = \frac{Qe^{-at}}{2\sqrt{\pi}} \mathrm{erf}\left[(L-x_0)/\sqrt{4Dt}\right]$$

The decay constant rate α in our problem can be assumed negligible, and therefore we set $\alpha = 0$, obtaining the following solution

$$\rho(x,t) = \frac{Q}{\sqrt{4\pi Dt}} e^{-(x-x_0)^2/4Dt} \tag{2}$$

$$Q_t(x,t) = \frac{Q}{2\sqrt{\pi}} \mathrm{erf}\left[(L-x_0)/\sqrt{4Dt}\right] \tag{3}$$

Let us first consider the boundary condition (b-1) which can be satisfied only applying the method of "reflection" and "superposition" [8, 11] by which the space charge density is expressed by two terms, where the second term constitutes the space charge density of a "virtual point charge" (image) at position $x = -x_0$. Therefore, the charge density is written

$$\rho(x,t) = \frac{Q}{\sqrt{4\pi Dt}} e^{-(x-x_0)^2/4Dt} + \frac{Q}{\sqrt{4\pi Dt}} e^{-(x+x_0)^2/4Dt} \tag{4}$$

Indeed, the boundary condition (b-1) at $x = 0$ is satisfied

$$\left.\frac{\partial \rho(x,t)}{\partial x}\right|_{x=0} = \left.\frac{Q}{\sqrt{4\pi Dt}} (-2)(x-x_0) e^{-(x-x_0)^2/4Dt} + \frac{Q}{\sqrt{4\pi Dt}} (-2)(x+x_0) e^{-(x+x_0)^2/4Dt}\right|_{x=0} = 0$$

For satisfying also the boundary condition (b2) we must introduce one more term for reflection and superposition with negative sign in this case. Therefore

$$\rho(x,t) = \frac{Q}{\sqrt{4\pi Dt}} e^{-(x-x_0)^2/4Dt} + \frac{Q}{\sqrt{4\pi Dt}} e^{-(x+x_0)^2/4Dt} - \frac{Q}{\sqrt{4\pi Dt}} e^{-(x-2L+x_0)^2/4Dt}$$

Based on this general solution we calculate the total charge as a function of space and time, where for simplicity we used 100 pC instead of the nominal one of 16 pC

$$Q_t(x,t) = \int_0^L \rho(x,t)\mathrm{d}x = \frac{Q}{\sqrt{4\pi Dt}} \int_0^L \left[e^{-(x-x_0)^2/4Dt} + e^{-(x+x_0)^2/4Dt} - e^{-(x-2L+x_0)^2/4Dt}\right] \mathrm{d}x$$

We also have

$$\int_0^L e^{-(x-x_0)^2/4Dt} \mathrm{d}x = \sqrt{4Dt} \int_{x_0/4Dt}^{(L-x_0)/4Dt} e^{-y^2} \mathrm{d}x = \sqrt{4Dt} \frac{\sqrt{\pi}}{2} \frac{2}{\sqrt{\pi}} \int_{-x_0/4Dt}^{(L-x_0)/4Dt} e^{-y^2} \mathrm{d}x$$

$$= \sqrt{4\pi Dt} \frac{1}{2} \left\{ \mathrm{erf}\left[(L-x_0)/\sqrt{4Dt}\right] - \mathrm{erf}\left(-x_0/\sqrt{4Dt}\right) \right\}$$

The total charge as a function of space-time including one image in the left side (Neumann boundary condition) and one image in the right side (Dirichlet boundary condition), is therefore reads as follows

$$Q_t(x,t) = \frac{Q}{2}\left\{\mathrm{erf}\left[(L-x_0)/\sqrt{4Dt}\right] - \mathrm{erf}\left(-x_0/\sqrt{4Dt}\right) + \mathrm{erf}\left[(L+x_0)/\sqrt{4Dt}\right] - \right.$$
$$\left. \mathrm{erf}\left(x_0/\sqrt{4Dt}\right) - \mathrm{erf}\left[(L-2L+x_0)/\sqrt{4Dt}\right] + \mathrm{erf}\left[(-2L+x_0)/\sqrt{4Dt}\right]\right\} \quad (5)$$

Nevertheless, the correct solution must be obtained by using the method of "reflection" and "superposition" including, theoretically, an infinite number of images of the actual point charge. In practice, a finite number of images can be used, however its number is unknown for a given accuracy. Especially, in the case we are studying (Neumann boundary condition at left end and Dirichlet at right end) greater number of images is necessary in order to avoid affecting the Neumann boundary condition at left for some individual cases, like deposited charge close to $x = L$ or/and at large times (of the order of 10 ms or higher in our application). Therefore, included an infinite number of images, we obtain

$$\rho(x,t) = \frac{Q}{\sqrt{4\pi Dt}} \sum_{m=-\infty}^{m=+\infty} (-1)^m \left[e^{-(x-2mL-x_0)^2/4Dt} + e^{-(x-2mL+x_0)^2/4Dt}\right] \quad (6)$$

where the index m counts the images except the value $m = 0$ which corresponds to the real point charge. The sign factor $(-1)^m$ has been used in order to change the sign of the image with respect to the right end where the Dirichlet boundary condition must be valid. In Fig. 2 a general graphical methodology for specifying the position of images given the position of the real point charge, is shown. A symbol of a positive Dirac function corresponds to the real point charge (red) while the other 8 Dirac functions corresponding to images (for $m = \pm 1, \pm 2$ left and right) are created by using successive conceivable closed paths (dashed lines). The different colors help for better understanding the image configuration while the transition signs in the crossing bullets provide the rule of specify the sign of the corresponding Dirac function.

Calculations of the total charge for the deposited charge at various points along the strip have been done by using software codes written in Matlab [12] as well as in Mathematica [13], out of the real deposited point charge, 12 pairs of images were included. Two time regions were used and the corresponding results shown in Fig. 3. Additionally, in Fig. 4 the family curves representing the total charge as a function of time in different positions of the point charge is shown. In Tables 1 and 2 the half-times as a function of the charge position for two values of resistivity are given.

Position x_0 [cm]	Equivalent half-time [μs]
99.5	2
98	35
95	210
90	900
75	5500
50	20000

Table 1: The equivalent half-time in different charge positions and for resistivity $R = 8$ MΩ/cm.

Position x_0 [cm]	Equivalent half-time [μs]
99.5	5
98	90
95	550
90	2200
75	15000
50	45000

Table 2: The equivalent half-time in different charge positions and for resistivity $R = 20$ MΩ/cm.

Based on the total charge as a function of time, the farther from the right end the charge is deposited the longer time it stays at high levels. Surely, the decrease is due to the sink at the right end. On the contrary, at distances very close to the right end, the charge decreases very quickly. Using the lasting time τ' that we have proposed in section 2, based on Fig. 3, we obtain: for the position $x = L/2 = 50$ cm, an "equivalent decay time" $\tau' = 30$ ms, while for the position $x = 99.5$ cm an "equivalent decay time" of $\tau' = 3$ μs.

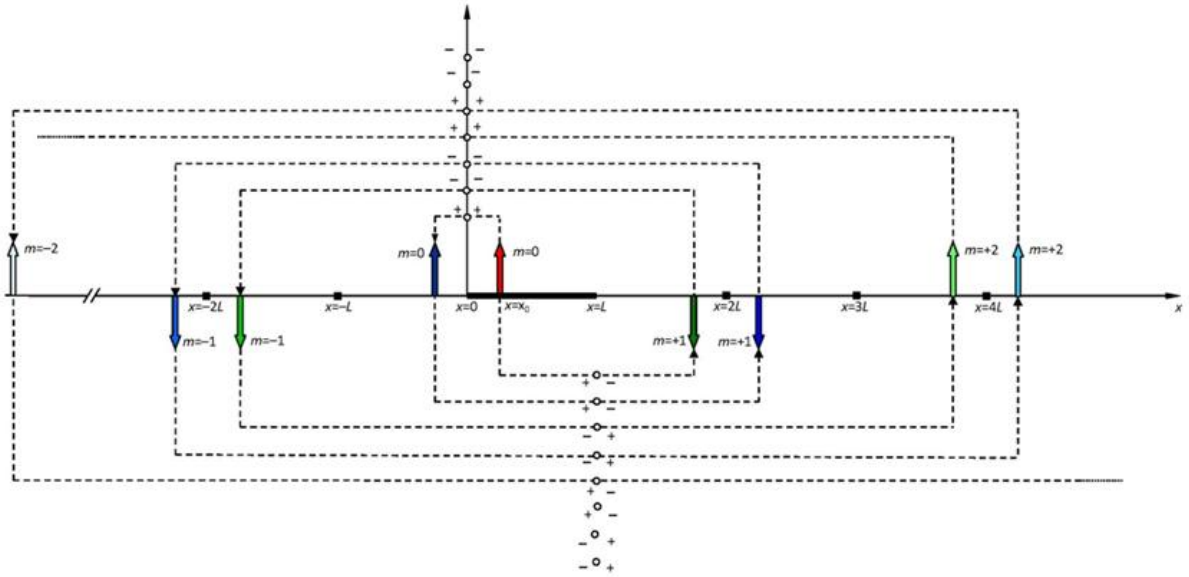

Figure 2: An indicative number of images, up to a second order, are represented schematically by their Dirac function together with the real point charge (red arrow) are shown. Starting from the red arrow a pair of images are created, a dark blue in the left and a dark green in the right. In turn, the dark blue image create another lighter blue in the right and a much lighter blue in the left. The green image creates a lighter green in the left and a much lighter in the right According to this methodology, we must always rotate counter-clockwise taking into account the marked alternation rule of the algebraic signs $(--, -+, +-, ++,)$ accordingly in each transition loop, from right to left and vice versa.

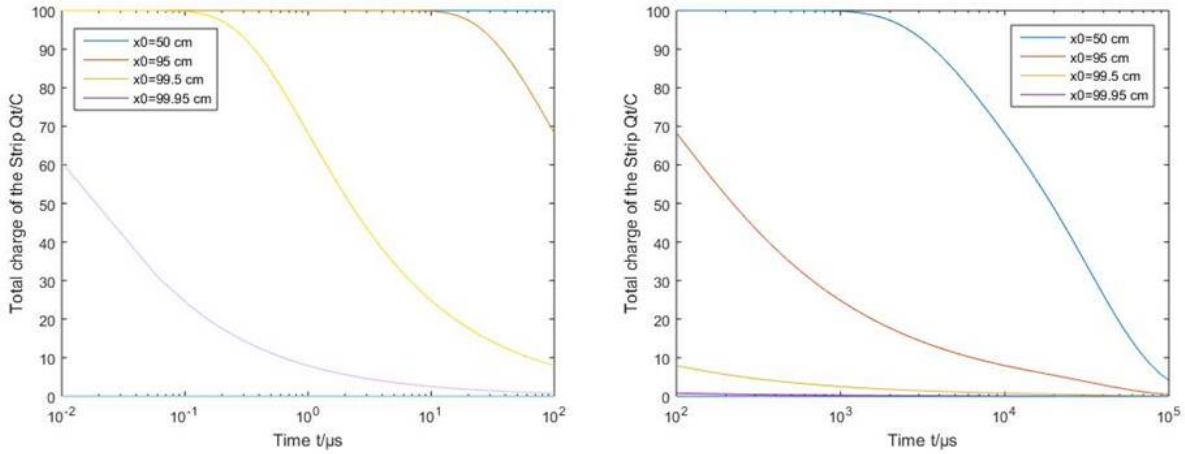

Figure 3: Total charge as a function of time in the range from 10 ns to 100 μs (left) and from 100 μs to 100 ms (right).

Let us now to calculate the electric field in the simplest case of an infinite one-dimensional resistive strip of infinitesimal width (like a "resistive wire"). Assuming the origin at the position of the deposited charge ($x' = 0$), we firstly calculate the electric potential in three dimensional space by integration. However, in this calculation we did not taken into account the presence of the metallic readout strip.

$$\Phi(\boldsymbol{r}, t) = \frac{1}{4\pi\varepsilon_0} \int_{-\infty}^{+\infty} \frac{\rho(x', t)}{|\boldsymbol{r} - \boldsymbol{x}'|} \mathrm{d}x' = \frac{Q}{4\pi\varepsilon_0\sqrt{4\pi Dt}} \int_{-\infty}^{+\infty} \frac{e^{-x'^2/4Dt}}{\sqrt{(\boldsymbol{r} - \boldsymbol{x}')^2 + y^2 + z^2}} \mathrm{d}x' \tag{7}$$

where $\boldsymbol{r}$ is the position vector in space and x' the position along the strip line. The electric field can

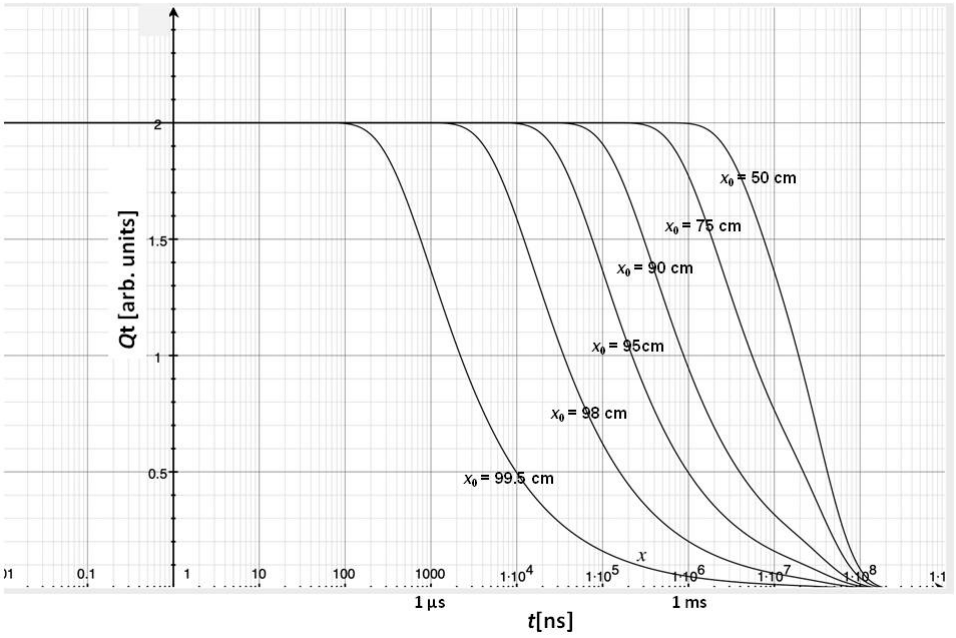

Figure 4: Total charge as a function of time in different positions of the point charge x_0. A resistivity of $R = 8$ MΩ/cm was assumed.

be calculated from Eq. 7 by using the gradient

$$\boldsymbol{E}(\boldsymbol{r}, t) = -\nabla \Phi(\mathbf{r}, t)$$

Now we consider a strip of finite length (from $x' = 0$ to $x' = L$) and of infinitesimal width to study again the space-time charge density of a deposited point charge at $x = x_0$. In this case the electric potential should be

$$\begin{aligned}
\Phi(\mathbf{r}, t; x_0) &= \frac{Q}{4\pi\varepsilon_0\sqrt{4\pi Dt}} \int_0^L \frac{\mathrm{d}x'}{|\boldsymbol{r} - \boldsymbol{x}'|} \sum_{m=-\infty}^{m=+\infty} (-1)^m \left[e^{-(x'-2mL-x_0)^2/4Dt} + e^{-(x'-2mL+x_0)^2/4Dt} \right] \\
&= \frac{Q}{4\pi\varepsilon_0\sqrt{4\pi Dt}} \int_0^L \frac{\mathrm{d}x'}{\sqrt{(x-x')^2 + y^2 + z^2}} \sum_{m=-\infty}^{m=+\infty} (-1)^m \left[e^{-(x'-2mL-x_0)^2/4Dt} + e^{-(x'-2mL+x_0)^2/4Dt} \right] \\
&= \frac{Q}{4\pi\varepsilon_0\sqrt{4\pi Dt}} \left[\sum_{m=-\infty}^{m=+\infty} \int_0^L \frac{(-1)^m e^{-(x'-2mL-x_0)^2/4Dt}}{\sqrt{(x-x')^2 + y^2 + z^2}} \mathrm{d}x' + \sum_{m=-\infty}^{m=+\infty} \int_0^L \frac{(-1)^m e^{-(x'-2mL+x_0)^2/4Dt}}{\sqrt{(x-x')^2 + y^2 + z^2}} \mathrm{d}x' \right]
\end{aligned} \tag{8}$$

and respectively, the electric field as a function in space-time with a parameter which is the position of the deposited pint-like charge, $x = x_0$, is obtained by

$$\boldsymbol{E}(\boldsymbol{r}, t; x_0) = -\nabla \Phi(\mathbf{r}, t; x_0) \tag{9}$$

In Fig. 5 the electric field as a function of time is shown for two cases of resistivity, $R = 8$ MΩ/cm and $R = 20$ MΩ/cm, respectively. The position of the deposited point charge along the strip is used as a parameter.

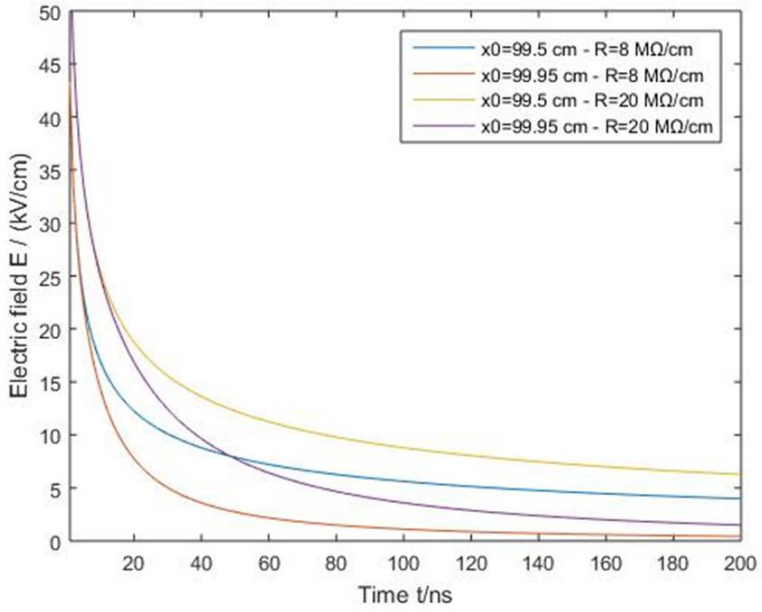

Figure 5: The electric field as a function of time at a vertical distance of 128 μm above different point charge positions $x = x_0$ (along z-axis, perpendicular to xy-plane). The curves include also the results for different values of resistivity.

3 Space-time diffusion along 2-D strip

3.1 Formulation of the 2-D problem

Let us now to consider a two-dimensional problem, that is, a point charge deposited to a strip of length L and width W, where $W \ll L$. In this case, the mechanism is governed by the 2-D diffusion-like equation, assuming $D_x = D_y = D$ given below

$$\frac{\partial \rho(x,y,t)}{\partial t} = D\frac{\partial^2 \rho(x,y,t)}{\partial x^2} + D\frac{\partial^2 \rho(x,y,t)}{\partial y^2} \tag{10}$$

Its general solution, in form of separation of variables (appropriate for a closed system), referring to the surface distribution of charge (charge per unit area) is

$$\sigma(x,y,t) = \frac{Q}{4\pi Dt} e^{-(x-x_0)^2/4Dt} \cdot e^{-y^2/4Dt} = \frac{Q}{4\pi Dt} e^{-\left[(x-x_0)^2+y^2\right]/4Dt} \tag{11}$$

3.2 Solutions for the 2-D problem

In this 2-D problem the initial condition is the same as in the 1-D problem while the boundary conditions are written separately for x and y variable. Therefore, the initial and the boundary conditions for this 2-D PDE, assuming the origin of y axis ($y = 0$) to be in the symmetry axis of the resistive strip, are

a) Initial condition for $t = 0$

   1) $\sigma(x,y,0) = Q\delta(x - x_0)\delta(y)$

b) Boundary conditions at left, right, lower and upper ends

   1) $\left.\frac{\partial \sigma(x,y,t)}{\partial x}\right|_{x=0} = 0$ (Neumann)
   2) $\sigma(x,y,t)|_{x=L} = \sigma(L,y,t) = 0$ (Dirichlet)
   3) $\left.\frac{\partial \sigma(x,y,t)}{\partial y}\right|_{y=-W/2} = 0$ (Neumann)

4) $\left.\frac{\partial\sigma(x,y,t)}{\partial y}\right|_{y=+W/2} = 0$ (Neumann)

As a first approximation we consider a uniform linear distribution of the charge along the y-direction (from $-W/2$ to $W/2$) before it starts diffusing along the x-axis. This is a realistic hypothesis because of the small width of the strip compared to its length. In other words, we assume that the perpendicular spread of the point charge happens instantaneously along y-direction leading to a uniform distribution. In this case we should have

$$\sigma(x,t) = \frac{1}{W}\frac{Q}{\sqrt{4\pi Dt}}e^{-(x-x_0)^2/4Dt} \tag{12}$$

where the factor $1/W$ is used for normalizing the charge. In turn, the corresponding potential including the associated images along the x-direction becomes

$$\Phi(\mathbf{r},t;x_0) = \frac{Q}{4\pi\varepsilon_0 W\sqrt{4\pi Dt}}\left[\sum_{m=-\infty}^{m=+\infty}\iint_{A'=L\cdot W}\frac{(-1)^m e^{-(x'-2mL-x_0)^2/4Dt}}{\sqrt{(x-x')^2+(y-y')^2+z^2}}\mathrm{d}x'\mathrm{d}y' + \right.$$
$$\left. + \sum_{m=-\infty}^{m=+\infty}\iint_{A'=L\cdot W}\frac{(-1)^m e^{-(x'-2mL+x_0)^2/4Dt}}{\sqrt{(x-x')^2+(y-y')^2+z^2}}\mathrm{d}x'\mathrm{d}y'\right] \tag{13}$$

In Fig. 6 the electric field, the component E_z due to the axis symmetry, as a function of time is calculated according to Eq. 8 and is shown for resistivity, 8 MΩ/cm and a width of the strip $W = 300$ μm assuming a deposited point charge at two different positions.

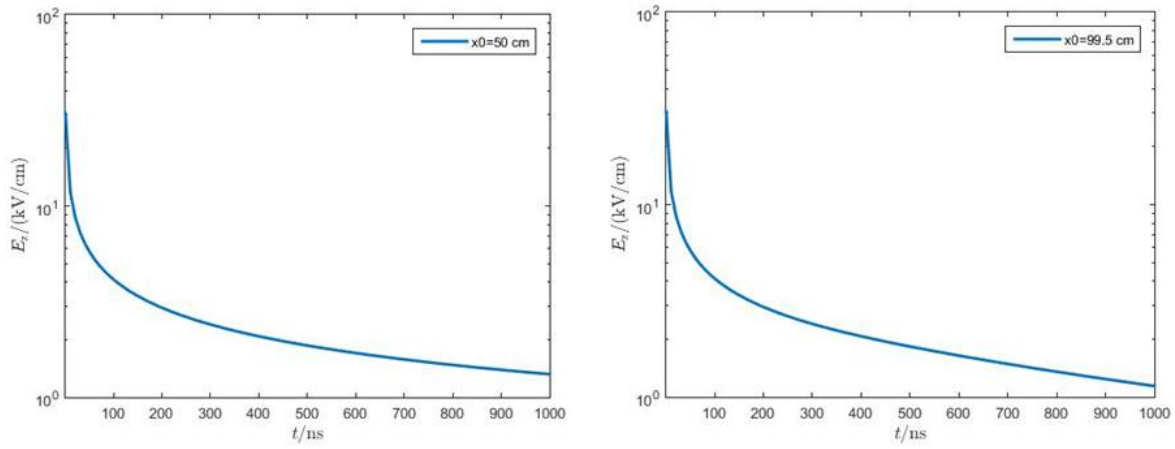

Figure 6: The electric field as a function of time in log scale, at vertical distance of 128 μm above the position $x = x_0$ (along the z-axis, perpendicular to xy-plane). The point charge is assumed to be deposited at $x_0 = 50$ cm (left) and $x_0 = 99.5$ cm (right). Two pairs of images, resistive $R = 8$ MΩ/cm and strip width of 300 μm were used in both cases.

In the most general consideration of a space-time spread along y-direction, at least two images must be included in the solution corresponding to the two boundary conditions (of Neumann type). Starting from the basic expression of the solution (of separated variables) for surface charge density expressed in charge per unit area, we have

$$\sigma(x,y,t) = \frac{Q}{4\pi Dt}e^{-(x-x_0)^2/4Dt}\left[e^{-y^2/4Dt} + e^{-(y+W)^2/4Dt} + e^{-(y-W)^2/4Dt}\right] \tag{14}$$

This solution includes the actual deposited charge diffused in x-direction for any y position and also two images, at lower and upper end of the strip, at distances equal to the width W for any x.

The general expression of the electric potential introducing infinite terms of images along x and y directions is

$$\Phi\left(\mathbf{r},t;x_0\right)=\frac{Q}{16\pi^2\varepsilon_0 Dt}\int_0^L\int_{-W/2}^{+W/2}\sum_{m=-\infty}^{m=+\infty}\left[\frac{(-1)^m e^{-(x'-2mL-x_0)^2/4Dt}}{\sqrt{(x-x')^2+(y-y')^2+z^2}}+\frac{(-1)^m e^{-(x'-2mL+x_0)^2/4Dt}}{\sqrt{(x-x')^2+(y-y')^2+z^2}}\right]\cdot \sum_{n=-\infty}^{n=+\infty}\frac{e^{-(y'-nW)^2/4Dt}}{\sqrt{(x-x')^2+(y-y')^2+z^2}}\mathrm{d}x'\mathrm{d}y' \quad (15)$$

The electric field is expected to be modified due to the 2-D spreading of the surface charge density, and thus, causing faster decreasing with time. In the more realistic case of 2-D strip consideration, the calculated electric field is decreased by time accordingly with the total charge. The impact of the resistivity to the spreading times, is that were suspected; the higher the resistivity the greater the spreading time, as it is seen in Fig. 5. The use of $R = 20$ MΩ/cm instead of $R = 8$ MΩ/cm increases the spreading times at the scale of 50%. Based on Fig. 6, for the position $x = L/2 = 50$ cm, the time for reduction of the electric field from the initial one (the point charge field) at 5% is about 85 ns, while for the position $x = 99.5$ cm is greater, about 95 ns. We conclude that the electric field is reduced very rapidly in both cases.

Conclusions and prospects

In the present work, the space-time spread of the deposited electric charge and the corresponding electric field in a resistive strip of the NSW Micromegas detectors were calculated analytically. The corresponding formulations have been derived and implemented by writing the particular software codes. In addition, an appropriate methodology was developed to find the sequence of the charge images that was necessary to get the solutions of the partial differential equations describing this phenomenon. Moreover, the created electric field has been calculated analytically helping to build its mapping in space as a function of time. The mechanism of initiating and developing of the sparks and how the counterbalance electric field contributes to their suppress, mostly in high particle rate environments, is an ongoing study.

Author Contributions

The authors contributed equally.

Funding

This research did not receive any specific grant from funding agencies in the public, commercial, or not-for-prodit sectors.

Data availability statement

This manuscript has no associated data or the data will not be deposited.

Declarations

Conflict of interest

The author has declared he has no conflict of interest with regard to this content.

Ethics

The author has declared ethics committee/IRB approval is not relevant to this content.

References

[1] ATLAS Collaboration, *ATLAS New Small Wheel Technical Design Report*, in the framework of ATLAS Phase I Upgrade, CERN-LHCC-2013-006, ATLAS TDR-20-2013.

[2] Y. Giomataris, Ph. Rebourgeard, J. P. Robert, G. Charpak, *MICROMEGAS: a high-granularity position-sensitive gaseous detector for high particle-flux environments*, Nuclear Instruments and Methods in Physics Research A 376 (1996) 29-35.

[3] Alexopoulos T et al. 2020 *Construction techniques and performances of a full-size prototype Micromegas chamber for the ATLAS muon spectrometer upgrade* Nuclear Instruments and Methods in Physics Research Section A 955 (2020) 162086.

[4] T. Alexopoulos et al., *A spark-resistant bulk-micromegas chamber for high rate applications*, Nuclear Instruments and Methods in Physics Research Section A,640 (2011) 110-118.

[5] M. S. Dixit1, A. Rankin, *Simulating the charge dispersion phenomena in Micro Pattern Gas Detectors with a resistive anode*, Nuclear Instruments and Methods in Physics Research A 566 (2006) 281285.

[6] M. S. Dixit2, J. Dubeau, J.-P. Martin and K. Sachs *Position Sensing from Charge Dispersion in Micro-Pattern Gas Detectors with a Resistive Anode*, Nuclear Instruments and Methods in Physics Research A 518 (2004) 721727.

[7] V. K. Srivastava, M. K. Awasthi, R. K. Chaurasia, and M. Tamsir, *The Telegraph Equation and Its Solution by Reduced Differential Transform Method*, Modelling and Simulation in Engineering, Volume 2013, Article ID 746351, http://dx.doi.org/10.1155/2013/746351.

[8] J. CRANK, *The Mathematics of Diffusion*, BRUNEL UNIVERSITY UXBRIDGE Second Edition, CLARENDON PRESS OXFORD (1975).

[9] W. Riegler, *Electric fields, weighting fields, signals and charge diffusion in detectors including resistive materials*, JINST 11 P11002, 2016.

[10] Marco Di Francesco, *Time-space population models: PDEs in biology*, Course notes, 2018.

[11] Benoit Cushman-Roisin, *ENVIRONMENTAL TRANSPORT AND FATE*, THAYER SCHOOL OF ENGINEERING DARTMOUTH COLLEGE HANOVER, NH 03755-8000 USA, Course notes, 2012.

[12] Mathworks, MATLAB R2015a; 2015.

[13] Mathematica 10.0 for Microsoft Windows (64-bit), Wolfram Research, Inc., 2014.